Enantiopure C 1 -Cyclotriveratrylene with a Reversed Spatial Arrangement of the Substituents

Augustin Long, Cédric Colomban, Marion Jean, Muriel Albalat, Nicolas Vanthuyne, Michel Giorgi, Lorenzo Di Bari, Marcin Górecki, Jean-Pierre Dutasta, Alexandre Martinez

Enantiopure C_1-Cyclotriveratrylene with a Reversed Spatial Arrangement of the Substituents

Long, A.
Colomban, C.
Jean, M.
Albalat, M.
Vanthuyne, N.
Giorgi, M.
Di Bari, L.
Gorecki, M.
Dutasta, J. P.
Martinez, A.

ABSTRACT: Cyclotriveratrylene (CTV) is a macrocyclic cyclophane presenting a bowl-shaped conformation, used as building block to construct cryptophane and hemi-cryptophane capsules. A method to synthesize new enantiopure CTV derivatives with an unprecedented spatial arrangement of their substituents, exhibiting C_1 symmetry, is described. The absolute configuration was assigned by ECD spectroscopy coupled with modeling. A statistical model has allowed for optimization of the proportion of C_1 CTV, and the modularity of this approach is also highlighted.

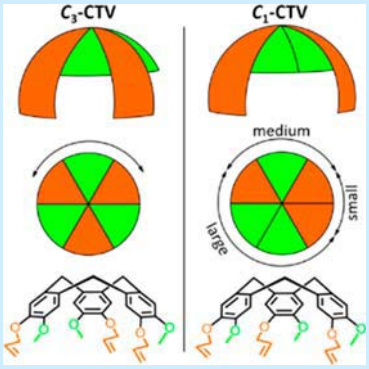

Cyclotriveratrylene (CTV) **1** is a macrocyclic trimer of veratrole presenting a bowl-shaped conformation (Figure 1a).[1] The first synthesis of the CTV was achieved independently by Ewins and Robinson in 1909 and 1915, respectively.[2] In 1965, Lindsey, Erdtman, and Goldup proposed a revised structure describing a macrocyclic trimer of aromatic rings.[3] Since then, various CTV analogues have been obtained by changing the nature of the R_1/R_2 substituents at their side arms (**2**, Figure 1b).[1] When R_1 differs from R_2, the CTV derivatives are chiral, and the resulting racemic mixture can be resolved.[4] Members of the CTV family have attracted considerable attention due to their usefulness for versatile applications ranging from separations,[5] sensing,[6] gels,[7] and dendrimers[8] to liquids crystals.[9] Moreover, they have been also used as building blocks for the construction of supramolecular assemblies such as polymers,[10] cubes,[11] pseudorotaxanes,[12] catenanes[13] and capsules.[1,14] In particular, the combination of two CTV derivatives, linked together, gives molecular capsules, named cryptophanes,[14,15] which present remarkable recognitions properties toward small molecules like epoxydes and methane,[16,17] cations like choline and cesium, and anions.[18,19] They were also found to complex Xe atom,[20] leading to promising tools for bioimaging.[21] When the CTV moiety is connected with another C_3 symmetrical unit, it gives rise to hemicryptophanes.[22] These chiral covalent cages can act as receptors for neurotransmitters and carbohydrates,[23,24] molecular switches,[25] and supramolecular catalysts.[26]

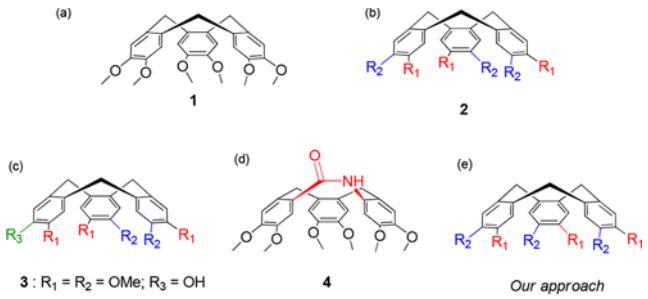

Figure 1. (a) Structure of the cyclotriveratylene **1**. (b) General structure of chiral CTV derivatives **2** with C_3 symmetry ($R_1 \neq R_2$). (c) Classical approach to obtain C_1 CTV derivatives. (d) Strategy of Becker et al.[27d] (e) Our approach.

While most CTV or CTV-based hosts reported so far present a C_3 symmetry, few C_1-symmetrical CTVs have been described in the literature.[27] This change of the symmetry results from the introduction of an R_3 group, different from R_1 and R_2, on one of the aromatic rings, for instance, by

monodemethylation of the CTV unit (compound **3**, Figure 1c) or by monoiodation of a C_3 CTV derivative.[27b,c] Becker et al. have recently reported the synthesis of the C_1 CTV-lactam **4** through the original functionalization of one of the apical position of the CTV moiety (Figure 1d).[27d] However, compound **4** turns out to be more flexible than the "classical" CTV moiety, leading to a lower energy barrier of racemization and avoiding their resolution by chiral HPLC. To the best of our knowledge, the straightforward synthesis of C_1-symmetrical CTV derivatives, where the loss of symmetry arises from the permutation of the substituents R_1 and R_2 (Figure 1e) on one of the aromatic ring is currently rather uncommon.[27e] Importantly, such an approach will lead to C_1-derivatives with an original spatial arrangement of their substituents, which will be highly valuable in order to access to cryptophanes and hemicryptophanes with shapes and sizes of their cavity that cannot be achieved by the existing methods.

Herein, we propose a new C_1 CTV structure where the loss of symmetry is due to an inverted arrangement of one aromatic ring. The unmodified CH_2 bridges, found in this structure, aim at maintaining its conformational rigidity, allowing for its resolution; meanwhile the specific arrangement of the substituents could afford a new chiral cyclophane building block, with a bowl-shaped conformation. We therefore report the synthesis of a CTV derivative, where the sequential distribution of the R_1/R_2 substituents is reversed on one of the aromatic ring (Figure 1e). To favor the formation of the C_1 over the C_3 CTV, we optimized the reaction conditions by mean of a statistical model. The racemic mixture was resolved by chiral HPLC and the assignment of the absolute configuration was achieved by ECD spectroscopy. Other related C_1 CTVs were prepared to highlight the modularity of our approach and X-ray diffraction analyses confirm the proposed structures.

C_1 CTV **5** bearing allyl and bromoethyl substituents was synthesized by mixing the two regio-isomers **6** and **7** in a 4:1 ratio in acetonitrile using scandium triflate as Lewis acid catalyst (Scheme 1). A mixture of C_3- and C_1-symmetric CTVs

Scheme 1. Synthesis of C_1 CTV 5[a]

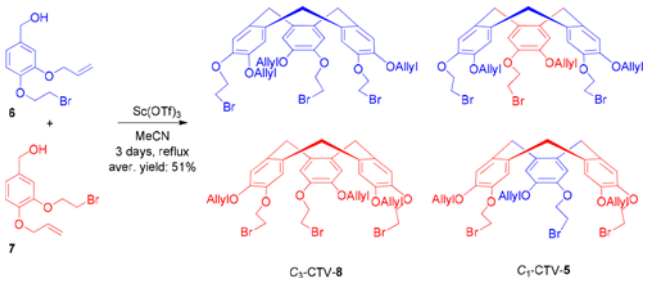

[a]A mixture of four stereoisomers is obtained: (+)-**8**, (−)-**8**, (+)-**5**, and (−)-**5**.

8 and **5**, respectively, was obtained in 52% yield after removal of the byproducts of the reaction (oligomers and polymers) by column chromatography. The four isomers (+)-**8**, (−)-**8**, (+)-**5**, and (−)-**5** were separated on chiral HPLC (see Figures S76 and 77), allowing isolation of each enantiomer of the CTV **5** on a gram scale. Both compounds **8** and **5** display identical mass spectra (Figures S56−S57); however the ^{1}H NMR spectrum of enantiopure CTV **8** confirms the C_3 symmetry, whereas that of enantiopure **5** exhibits a more complex pattern (Figures S26 and S28). For instance, the characteristic signals corresponding to the H_a protons of the AB systems of the CH_2 bridges in **5** appear as the superposition of three doublets at 4.71 ppm, with an expected coupling constant around 13.6 Hz, and the aromatic protons of the three CTV units give six singlets between 6.85 and 6.95 ppm.

The chiroptical properties of the two enantiomers of **5** were then studied. Their optical rotations, measured in CH_2Cl_2 at 589 nm, correspond to a third of that of their C_3 parents (±5 and ±15 deg cm^2 g^{-1}, respectively (see the Supporting Information)). Similarly, their electronic circular dichroism (ECD) spectra, recorded in MeCN at 25 °C (Figures 2 and

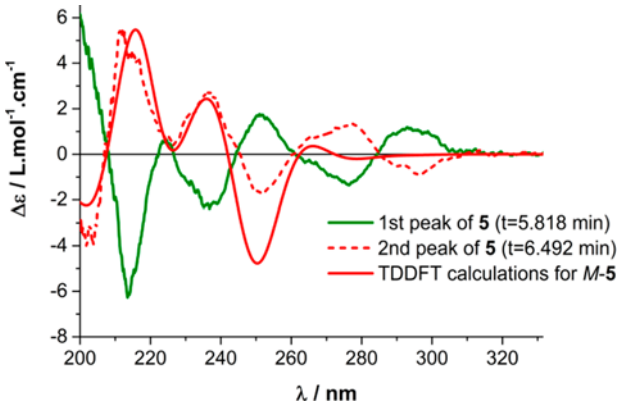

Figure 2. Experimental ECD spectra of the enantiomers of **5**: the first eluted enantiomer is represented with a green solid line (0.404 mmol L^{-1} in CH_2Cl_2) and the second one by a red dotted line (0.442 mmol L^{-1} in CH_2Cl_2) together with TDDFT calculations performed for *M*-**5**. Calculations were carried out at the CAM-B3LYP/SVP/PCM-(MeCN) level of theory; spectrum red-shifted by 33 nm, Gaussian bandwidth 0.23 eV, similarity factor assigned by means of SpecDis ver. 1.70 for the second peak = 0.833, while for the first one = 0.008.[30]

Figures S94 and S95), also exhibit a decrease of the intensities for the observed transitions by two-thirds compared to their C_3 counterparts. The inverted position of one of the aromatic rings probably induces two excitons coupling of the same sign and one of the opposite and could account for this experimental result. The assignment of the absolute configuration of the C_1 CTV was then achieved. First, the stereodescriptor was chosen according to the method described by Prelog.[28] However, because of the lack of the C_3 axis, the conformations around the six CH_2−Ar single bonds are no more equivalent. The priority of one pair can be determined according to CIP rules, and the procedure of Prelog can be applied, giving a *M* descriptor, if $R_1 > R_2$, for the enantiomer drawn in Figure 1e (see the Supporting Information for more details).[28] Second, this stereodescriptor was linked with a chiroptical property so that their electronic circular dichroism (ECD) spectra were thus used to achieve this goal. Indeed, the spectra exhibit two exciton patterns centered on the isotropic absorption of the ^1L_a (~240 nm) and ^1L_b (~290 nm) transitions, as usually observed for CTV analogues. Collet et al. have demonstrated that the sign of the bands of the experimental ECD spectrum around the ^1L_a ~ 240 nm is poorly sensitive to the nature of CTV derivatives substituents. Therefore, the determination of their absolute configuration was achieved by means of comparison to the calculated ECD spectra of a reference CTV.[29] On the basis of these previous works, the second and third eluted compounds

((+)-**5** and (−)-**5**, respectively) correspond to the *P* and *M* configurations, whereas the first and fourth eluted compounds ((+)-**8** and (−)-**8**, respectively) correspond to the *P* and *M* configurations of the C_3 CTV. To confirm this stereochemical assignment, ECD spectra were calculated for an arbitrary chosen *M*-**5** by using the TDDFT method. In order to guarantee the quality of the obtained data, two hybrid functionals (CAM-B3LYP, ωB97X-D) with the SVP basis set and PCM model for MeCN were tested. The results are completely in agreement. This confirms the aforementioned assignment; i.e., the second eluted peak is *M*-**5**, while the first one is *P*-**5** (Figure 2).

We then focused our attention on the improvement of the C_1/C_3 ratio (**5**/**8** ratio) by varying the initial proportions of the starting regioisomers **6** and **7**. The proportions of C_3 and C_1 CTV derivatives can be explained by a simple statistical model, assuming (i) a kinetic model for the reaction, (ii) that both isomers **6** and **7** have the same reactivity, and (iii) that the racemization of the CTVs C_1 and C_3 occurs frequently during the reaction time (see the Supporting Information). This latter hypothesis was assessed by measuring the energy barrier of the C_1 enantiomer. A value of 112.1 kJ mol^{-1} was found, similar to that of its C_3 parent, which corresponds to a half-life time of 24 min at 82 °C (Figures S100 and S101). With this model for the cyclization, the probabilities are given by the polynomial law with Newton's binomial coefficients

$$P_{C_3}(x) = \binom{3}{0}x^0(1-x)^{3-0} + \binom{3}{3}x^3(1-x)^{3-3} = 1 - 3x(1-x)$$

$$P_{C_1}(x) = \binom{3}{1}x^1(1-x)^{3-1} + \binom{3}{2}x^2(1-x)^{3-2} = 3x(1-x)$$

where x is the proportion of regioisomer and $P_{C_1}(x)$ and $P_{C_3}(x)$ the probabilities to obtain the C_1 and C_3 CTV, respectively. Thus, from these equations we find that the maximum of the function P_{C_1} is reached for an equimolar mixture of each regioisomer (x = 0.5) and yields a maximum of 75% of C_1 derivative and 25% of C_3 derivative. To confirm this model, several cyclizations were performed under the same conditions with different proportions x of the starting regioisomer **7**. The proportions P_{C_1} and P_{C_3} were both determined by ^{1}H NMR and HPLC (Figures S65−S74). The statistical model was found to be in excellent agreement with the experiments, confirming our hypothesis (Figure 3). Moreover, it supports that the optimal conditions for the synthesis of C_1 derivative

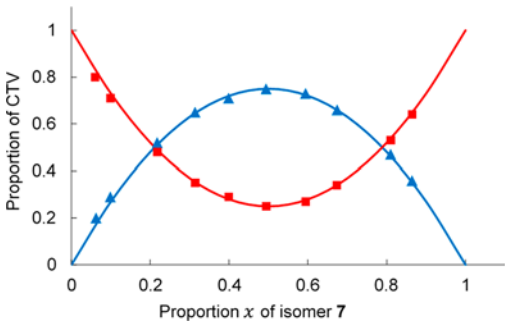

Figure 3. Proportion of C_3 CTV-**8** (in red) and C_1 CTV-**5** (in blue) obtained with different initial proportions x of isomer **7** for the cyclization. Triangles represent the experimental proportions, and the line represents the binomial statistical model.

are reached when an equimolar mixture of both isomers is used, leading to a maximum yield of 75% of C_1 CTV.

We then examined if other C_1 CTV derivatives, presenting an inverted arrangement of one of their aromatic rings, could be obtained following our method. Using the same procedure and starting from the 1:1 mixture of the two regioisomers **11** and **12**, a mixture of C_3 and C_1 CTV **9** was obtained in 46% yield, with a C_3/C_1 ratio of 25/75 in agreement with the previously established statistical model. The subsequent deprotection of the allyl groups then affords the C_3 and C_1 CTV **10** in 90% yield (Scheme 2). Resolution of CTVs **9** and

Scheme 2. Synthesis of C_1 CTV-9 and -10

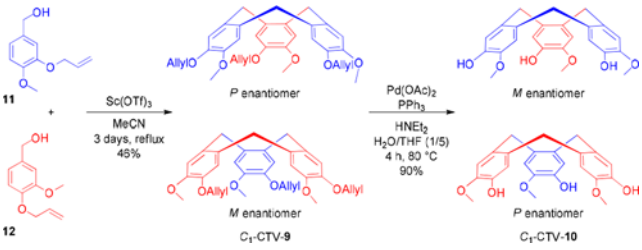

10 was performed on chiral HPLC (see the Supporting Information). As previously observed with CTV-**5**, the chiroptical properties of the C_1 CTVs **9** and **10** are one-third of those of their C_3 parents. The absolute configurations of these C_1 CTVs were assigned using the same strategy as that described for C_1 CTV **5**. Furthermore, it should be noted that various functional groups can be easily grafted on the phenol function of C_1 CTV **10**, allowing for a straightforward tuning of its properties and making it a promising cyclophane building block. Single crystals suitable for X-ray diffraction studies of C_1 CTV-**9** and C_1 CTV-**10** were obtained by slow diffusion of pentane and ether, respectively, in chloroform solutions (Figure 4 and Figures S104 and 105). These compounds

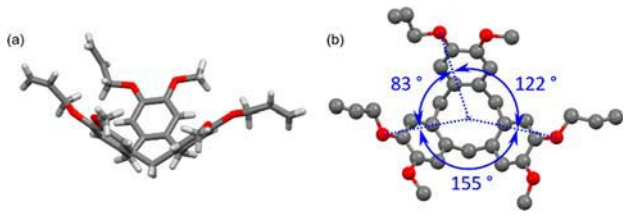

Figure 4. (a) X-ray crystal structure of (−)-*P*−C_1 CTV-**9**. (b) Angles between the bulky linkers.

display the expected bowl-shaped structure, with the permutation of the spatial arrangement of the substituents on one of the aromatic rings. The angles formed between the oxygen atoms bearing the bulky substituents and their barycenter are reported in Figure 4b, highlighting the difference between the three intervals, induced by the desymmetrization.

We have thus described the unprecedented synthesis of enantiopure C_1-symmetrical CTVs. The C_3 symmetry, classically observed with CTV derivatives, was successfully broken following a novel approach based on the inversion of the position of the two alkoxy groups of one of the aromatic rings. This leads to original enantiopure bowl-shaped cyclophanes with novel structural and optical properties. Importantly, the C_1 CTV scaffold obtained following this approach

represents a new tool for the construction of molecular cages with three apertures of different sizes. In addition, this is a promising strategy for the fine-tuning of the in/out kinetics of guest encapsulation inside the cryptophane cavity, while retaining high affinity. As the C_1 CTVs precursors can be easily obtained in a gram scale, we envision that library of such challenging building blocks can be rapidly built.

(1) (a) Hardie, M. J. Recent Advances in the Chemistry of Cyclotriveratrylene. *Chem. Soc. Rev.* **2010**, *39*, 516−527. (b) Collet, A. Cyclotriveratrylenes and Cryptophanes. *Tetrahedron* **1987**, *43*, 5725−5759.

(2) (a) Robinson, G. M. A Reaction of Homopiperonyl and of Homoveratryl Alcohols. *J. Chem. Soc., Trans.* **1915**, *107*, 267−276. (b) Ewins, A. J. The Action of Phosphorus Pentachloride on the Methylene Ethers of Catechol Derivatives. Part V. Derivatives of Protocatechuyl Alcohol and Protocatechuonitrile. *J. Chem. Soc., Trans.* **1909**, *95*, 1482−1488.

(3) (a) Lindsey, A. S. The Structure of Cyclotriveratrylene (10,15-Dihydro-2,3,7,8,12,13-Hexamethoxy-5H-Tribenzo[a,d,g]-Cyclononene) and Related Compounds. *J. Chem. Soc.* **1965**, *0*, 1685−1692. (b) Erdtman, H.; Haglid, F.; Ryhage, R. Macrocyclic Condensation Products of Veratrole and Resorcinol. *Acta Chem. Scand.* **1964**, *18*, 1249−1254. (c) Goldup, A.; Morrison, A. B.; Smith, G. W. The Effect of Sodium Tungstate Additions on the Thermal Dehydration of Silica Xerogel. *J. Chem. Soc., Res.* **1965**, 3854−3904.

(4) Lefevre, S.; Héloin, A.; Pitrat, D.; Mulatier, J.-C.; Vanthuyne, N.; Jean, M.; Dutasta, J.-P.; Guy, L.; Martinez, A. Cyclotriveratrylene-BINOL-Based Host Compounds: Synthesis, Absolute Configuration Assignment, and Recognition Properties. *J. Org. Chem.* **2016**, *81*, 3199−3205.

(5) (a) Ku, M.-Y.; Huang, S.-J.; Huang, S.-L.; Liu, Y.-H.; Lai, C.-C.; Peng, S.-M.; Chiu, S.-H. Hemicarceplex Formation Allows Ready Identification of the Isomers of the Metallofullerene Sc_3N@C80 Using ^{1}H and ^{13}C NMR Spectroscopy. *Chem. Commun.* **2014**, *50*, 11709−11712. (b) Feng, L.-J.; Li, H.; Chen, Q.; Han, B.-H. Cationic Cyclotriveratrylene-Based Glycoconjugate and Its Interaction with Fullerene. *RSC Adv.* **2013**, *3*, 6985−6990. (c) Wang, L.; Wang, G.-T.; Zhao, X.; Jiang, X.-K.; Li, Z.-T. Hydrogen Bonding-Directed Quantitative Self-Assembly of Cyclotriveratrylene Capsules and Their Encapsulation of C_{60} and C_{70}. *J. Org. Chem.* **2011**, *76*, 3531−3535. (d) Huerta, E.; Isla, H.; Pérez, E. M.; Bo, C.; Martín, N.; Mendoza, J. de. Tripodal ExTTF-CTV Hosts for Fullerenes. *J. Am. Chem. Soc.* **2010**, *132*, 5351−5353. (e) Lijanova, I. V.; Maturano, J. F.; Chávez, J. G. D.; Montes, K. E. S.; Ortega, S. H.; Klimova, T.; Martínez-García, M. Synthesis of Cyclotriveratrylene Dendrimers and Their Supramolecular Complexes with Fullerene C_{60}. *Supramol. Chem.* **2009**, *21*, 24−34.

(6) (a) Erieau-Peyrard, L.; Coiffier, C.; Bordat, P.; Bégué, D.; Chierici, S.; Pinet, S.; Gosse, I.; Baraille, I.; Brown, R. Selective, Direct Detection of Acetylcholine in PBS Solution, with Self-Assembled Fluorescent Nano-Particles: Experiment and Modelling. *Phys. Chem. Chem. Phys.* **2015**, *17*, 4168−4174. (b) Sarsah, S. R. S.; Lutz, M. R.; Zeller, M.; Crumrine, D. S.; Becker, D. P. Rearrangement of Cyclotriveratrylene (CTV) Diketone: 9,10-Diarylanthracenes with OLED Applications. *J. Org. Chem.* **2013**, *78*, 2051−2058. (c) Peyrard, L.; Dumartin, M.-L.; Chierici, S.; Pinet, S.; Jonusauskas, G.; Meyrand, P.; Gosse, I. Development of Functionalized Cyclotriveratrylene Analogues: Introduction of Withdrawing and π-Conjugated Groups. *J. Org. Chem.* **2012**, *77*, 7023−7027.

(7) (a) Westcott, A.; Sumby, C. J.; Walshaw, R. D.; Hardie, M. J. Metallo-Gels and Organo-Gels with Tripodal Cyclotriveratrylene-Type and 1,3,5-Substituted Benzene-Type Ligands. *New J. Chem.* **2009**, *33*, 902−912. (b) Bardelang, D.; Camerel, F.; Ziessel, R.; Schmutz, M.; Hannon, M. J. New Organogelators Based on Cyclotriveratrylene Platforms Bearing 2-Dimethylacetal-5-Carbonylpyridine Fragments. *J. Mater. Chem.* **2008**, *18*, 489−494.

(8) Percec, V.; Imam, M. R.; Peterca, M.; Wilson, D. A.; Heiney, P. A. Self-Assembly of Dendritic Crowns into Chiral Supramolecular Spheres. *J. Am. Chem. Soc.* **2009**, *131*, 1294−1304.

(9) (a) Zimmermann, H.; Bader, V.; Poupko, R.; Wachtel, E. J.; Luz, Z. Mesomorphism, Isomerization, and Dynamics in a New Series of Pyramidic Liquid Crystals. *J. Am. Chem. Soc.* **2002**, *124*, 15286−15301. (b) Lunkwitz, R.; Tschierske, C.; Diele, S. Formation of Smectic and Columnar Liquid Crystalline Phases by Cyclotriveratrylene (CTV) and Cyclotetraveratrylene (CTTV) Derivatives Incorporating Calamitic Structural Units. *J. Mater. Chem.* **1997**, *7*, 2001−2011.

(10) (a) Thorp-Greenwood, F. L.; Ronson, T. K.; Hardie, M. J. Copper Coordination Polymers from Cavitand Ligands: Hierarchical Spaces from Cage and Capsule Motifs, and Other Topologies. *Chem. Sci.* **2015**, *6*, 5779−5792. (b) Thorp-Greenwood, F. L.; Berry, G. T.; Boyadjieva, S. S.; Oldknow, S.; Hardie, M. J. 2D Networks of Metallo-Capsules and Other Coordination Polymers from a Hexapodal Ligand. *CrystEngComm* **2018**, *20*, 3960−3970.

(11) (a) Fowler, J. M.; Thorp-Greenwood, F. L.; Warriner, S. L.; Willans, C. E.; Hardie, M. J. M12L8Metallo-Supramolecular Cube with Cyclotriguaiacylene-Type Ligand: Spontaneous Resolution of Cube and Its Constituent Host Ligand. *Chem. Commun.* **2016**, *52*, 8699−8702. (b) Xu, D.; Warmuth, R. Edge-Directed Dynamic Covalent Synthesis of a Chiral Nanocube. *J. Am. Chem. Soc.* **2008**, *130*, 7520−7521.

(12) Thorp-Greenwood, F. L.; Brennan, A. D.; Oldknow, S.; Henkelis, J. J.; Simmons, K. J.; Fishwick, C. W. G.; Hardie, M. J. Tris-N-Alkylpyridinium-Functionalised Cyclotriguaiacylene Hosts as Axles

in Branched [4]Pseudorotaxane Formation. *Supramol. Chem.* **2017**, *29*, 430−440.
(13) Westcott, A.; Fisher, J.; Harding, L. P.; Rizkallah, P.; Hardie, M. J. Self-Assembly of a 3-D Triply Interlocked Chiral [2]Catenane. *J. Am. Chem. Soc.* **2008**, *130*, 2950−2951.
(14) (a) El-Ayle, G.; Holman, K. T. Cryptophanes. In *Comprehensive Supramolecular Chemistry II*; Atwood, J. L., Gokel, G. W., Barbour, L. J., Eds.; Elsevier: New York, 2017. (b) Brotin, T.; Dutasta, J.-P. Cryptophanes and Their Complexes—Present and Future. *Chem. Rev.* **2009**, *109*, 88−130.
(15) (a) Henkelis, J. J.; Hardie, M. J. Controlling the Assembly of Cyclotriveratrylene-Derived Coordination Cages. *Chem. Commun.* **2015**, *51*, 11929−11943. (b) Henkelis, J. J.; Hardie, M. J. Tuning the Coordination Chemistry of Cyclotriveratrylene Ligand Pairs through Alkyl Chain Aggregation. *CrystEngComm* **2014**, *16*, 8138−8146. (c) Ronson, T. K.; Nowell, H.; Westcott, A.; Hardie, M. J. Bow-Tie Metallo-Cryptophanes from a Carboxylate Derived Cavitand. *Chem. Commun.* **2011**, *47*, 176−178. (d) Oldknow, S.; Martir, D. R.; Pritchard, V. E.; Blitz, M. A.; Fishwick, C. W. G.; Zysman-Colman, E.; Hardie, M. J. Structure-Switching M_3L_2 Ir(III) Coordination Cages with Photo-Isomerising Azo-Aromatic Linkers. *Chem. Sci.* **2018**, *9*, 8150−8159. (e) Kai, S.; Kojima, T.; Thorp-Greenwood, F. L.; Hardie, M. J.; Hiraoka, S. How Does Chiral Self-Sorting Take Place in the Formation of Homochiral Pd_6L_8 Capsules Consisting of Cyclotriveratrylene-Based Chiral Tritopic Ligands? *Chem. Sci.* **2018**, *9*, 4104−4108. (f) Cookson, N. J.; Fowler, J. M.; Martin, D. P.; Fisher, J.; Henkelis, J. J.; Ronson, T. K.; Thorp-Greenwood, F. L.; Willans, C. E.; Hardie, M. J. Metallo-Cryptophane Cages from Cis-Linked and Trans-Linked Strategies. *Supramol. Chem.* **2018**, *30*, 255−266. (g) Pritchard, V. E.; Rota Martir, D.; Oldknow, S.; Kai, S.; Hiraoka, S.; Cookson, N. J.; Zysman-Colman, E.; Hardie, M. J. Homochiral Self-Sorted and Emissive IrIII Metallo-Cryptophanes. *Chem. - Eur. J.* **2017**, *23*, 6290−6294. (h) Hardie, M. J. Self-Assembled Cages and Capsules Using Cyclotriveratrylene-Type Scaffolds. *Chem. Lett.* **2016**, *45*, 1336−1346. (i) Chapellet, L.-L.; Cochrane, J. R.; Mari, E.; Boutin, C.; Berthault, P.; Brotin, T. Synthesis of Cryptophanes with Two Different Reaction Sites: Chemical Platforms for Xenon Biosensing. *J. Org. Chem.* **2015**, *80*, 6143−6151. (j) Brégier, F.; Hudeček, O.; Chaux, F.; Penouilh, M.-J.; Chambron, J.-C.; Lhoták, P.; Aubert, E.; Espinosa, E. Generation of Cryptophanes in Water by Disulfide Bridge Formation. *Eur. J. Org. Chem.* **2017**, *2017*, 3795−3811. (k) Schaly, A.; Rousselin, Y.; Chambron, J.-C.; Aubert, E.; Espinosa, E. The Stereoselective Self-Assembly of Chiral Metallo-Organic Cryptophanes. *Eur. J. Inorg. Chem.* **2016**, *2016*, 832−843.
(16) Bouchet, A.; Brotin, T.; Linares, M.; Ågren, H.; Cavagnat, D.; Buffeteau, T. Enantioselective Complexation of Chiral Propylene Oxide by an Enantiopure Water-Soluble Cryptophane. *J. Org. Chem.* **2011**, *76*, 4178−4181.
(17) Garel, L.; Dutasta, J.-P.; Collet, A. Complexation of Methane and Chlorofluorocarbons by Cryptophane-A in Organic Solution. *Angew. Chem., Int. Ed. Engl.* **1993**, *32*, 1169−1171.
(18) (a) Brotin, T.; Goncalves, S.; Berthault, P.; Cavagnat, D.; Buffeteau, T. Influence of the Cavity Size of Water-Soluble Cryptophanes on Their Binding Properties for Cesium and Thallium Cations. *J. Phys. Chem. B* **2013**, *117*, 12593−12601. (b) Brotin, T.; Cavagnat, D.; Berthault, P.; Montserret, R.; Buffeteau, T. Water-Soluble Molecular Capsule for the Complexation of Cesium and Thallium Cations. *J. Phys. Chem. B* **2012**, *116*, 10905−10914. (c) Brotin, T.; Montserret, R.; Bouchet, A.; Cavagnat, D.; Linares, M.; Buffeteau, T. High Affinity of Water-Soluble Cryptophanes for Cesium Cations. *J. Org. Chem.* **2012**, *77*, 1198−1201.
(19) (a) Fairchild, R. M.; Holman, K. T. Selective Anion Encapsulation by a Metalated Cryptophane with a π-Acidic Interior. *J. Am. Chem. Soc.* **2005**, *127*, 16364−16365. (b) Fairchild, R. M.; Joseph, A. I.; Holman, K. T.; Fogarty, H. A.; Brotin, T.; Dutasta, J.-P.; Boutin, C.; Huber, G.; Berthault, P. A Water-Soluble Xe@ cryptophane-111 Complex Exhibits Very High Thermodynamic Stability and a Peculiar ^{129}Xe NMR Chemical Shift. *J. Am. Chem. Soc.* **2010**, *132*, 15505−15507.
(20) (a) Bartik, K.; Luhmer, M.; Dutasta, J.-P.; Collet, A.; Reisse, J. ^{129}Xe and ^{1}H NMR Study of the Reversible Trapping of Xenon by Cryptophane-A in Organic Solution. *J. Am. Chem. Soc.* **1998**, *120*, 784−791. (b) Boutin, C.; Léonce, E.; Brotin, T.; Jerschow, A.; Berthault, P. Ultrafast Z-Spectroscopy for ^{129}Xe NMR-Based Sensors. *J. Phys. Chem. Lett.* **2013**, *4*, 4172−4176. (c) Joseph, A. I.; Lapidus, S. H.; Kane, C. M.; Holman, K. T. Extreme Confinement of Xenon by Cryptophane-111 in the Solid State. *Angew. Chem., Int. Ed.* **2015**, *54*, 1471−1475. (d) Joseph, A. I.; El-Ayle, G.; Boutin, C.; Léonce, E.; Berthault, P.; Holman, K. T. Rim-Functionalized Cryptophane-111 Derivatives via Heterocapping, and Their Xenon Complexes. *Chem. Commun.* **2014**, *50*, 15905−15908.
(21) (a) Riggle, B. A.; Wang, Y.; Dmochowski, I. J. A "Smart" ^{129}Xe NMR Biosensor for PH-Dependent Cell Labeling. *J. Am. Chem. Soc.* **2015**, *137*, 5542−5548. (b) Witte, C.; Martos, V.; Rose, H. M.; Reinke, S.; Klippel, S.; Schröder, L.; Hackenberger, C. P. R. Live-Cell MRI with Xenon Hyper-CEST Biosensors Targeted to Metabolically Labeled Cell-Surface Glycans. *Angew. Chem., Int. Ed.* **2015**, *54*, 2806−2810. (c) Khan, N. S.; Riggle, B. A.; Seward, G. K.; Bai, Y.; Dmochowski, I. J. Cryptophane-Folate Biosensor for ^{129}Xe NMR. *Bioconjugate Chem.* **2015**, *26*, 101−109. (d) Rose, H. M.; Witte, C.; Rossella, F.; Klippel, S.; Freund, C.; Schröder, L. Development of an Antibody-Based, Modular Biosensor for ^{129}Xe NMR Molecular Imaging of Cells at Nanomolar Concentrations. *Proc. Natl. Acad. Sci. U. S. A.* **2014**, *111*, 11697−11702. (e) Kotera, N.; Tassali, N.; Léonce, E.; Boutin, C.; Berthault, P.; Brotin, T.; Dutasta, J.-P.; Delacour, L.; Traoré, T.; Buisson, D.-A.; Taran, F.; Coudert, S.; Rousseau, B. A Sensitive Zinc-Activated ^{129}Xe MRI Probe. *Angew. Chem., Int. Ed.* **2012**, *51*, 4100−4103. (f) Stevens, T. K.; Palaniappan, K. K.; Ramirez, R. M.; Francis, M. B.; Wemmer, D. E.; Pines, A. HyperCEST Detection of a ^{129}Xe-Based Contrast Agent Composed of Cryptophane-A Molecular Cages on a Bacteriophage Scaffold. *Magn. Reson. Med.* **2013**, *69*, 1245−1252. (g) Seward, G. K.; Bai, Y.; Khan, N. S.; Dmochowski, I. J. Cell-Compatible, Integrin-Targeted Cryptophane-^{129}XeNMR Biosensors. *Chem. Sci.* **2011**, *2*, 1103−1110. (h) Meldrum, T.; Seim, K. L.; Bajaj, V. S.; Palaniappan, K. K.; Wu, W.; Francis, M. B.; Wemmer, D. E.; Pines, A. A Xenon-Based Molecular Sensor Assembled on an MS2 Viral Capsid Scaffold. *J. Am. Chem. Soc.* **2010**, *132*, 5936−5937. (i) Tassali, N.; Kotera, N.; Boutin, C.; Léonce, E.; Boulard, Y.; Rousseau, B.; Dubost, E.; Taran, F.; Brotin, T.; Dutasta, J.-P.; Berthault, P. Smart Detection of Toxic Metal Ions, Pb^{2+} and Cd^{2+}, Using a ^{129}Xe NMR-Based Sensor. *Anal. Chem.* **2014**, *86*, 1783−1788. (j) Schröder, L.; Lowery, T. J.; Hilty, C.; Wemmer, D. E.; Pines, A. Molecular Imaging Using a Targeted Magnetic Resonance Hyperpolarized Biosensor. *Science* **2006**, *314*, 446−449.
(22) (a) Canceill, J.; Collet, A.; Gabard, J.; Kotzyba-Hibert, F.; Lehn, J.-M. Speleands. Macropolycyclic Receptor Cages Based on Binding and Shaping Sub-Units. Synthesis and Properties of Macrocycle Cyclotriveratrylene Combinations. Preliminary Communication. *Helv. Chim. Acta* **1982**, *65*, 1894−1897. (b) Zhang, D.; Martinez, A.; Dutasta, J.-P. Emergence of Hemicryptophanes: From Synthesis to Applications for Recognition, Molecular Machines, and Supramolecular Catalysis. *Chem. Rev.* **2017**, *117*, 4900−4942.
(23) Zhang, D.; Gao, G.; Guy, L.; Robert, V.; Dutasta, J.-P.; Martinez, A. A Fluorescent Heteroditopic Hemicryptophane Cage for the Selective Recognition of Choline Phosphate. *Chem. Commun.* **2015**, *51*, 2679−2682.
(24) (a) Zhang, D.; Mulatier, J.-C.; Cochrane, J. R.; Guy, L.; Gao, G.; Dutasta, J.-P.; Martinez, A. Helical, Axial, and Central Chirality Combined in a Single Cage: Synthesis, Absolute Configuration, and Recognition Properties. *Chem. - Eur. J.* **2016**, *22*, 8038−8042. (b) Long, A.; Perraud, O.; Albalat, M.; Robert, V.; Dutasta, J.-P.; Martinez, A. Helical Chirality Induces a Substrate-Selectivity Switch in Carbohydrates Recognitions. *J. Org. Chem.* **2018**, *83*, 6301−6306.
(25) (a) Zhang, D.; Cochrane, J. R.; Di Pietro, S.; Guy, L.; Gornitzka, H.; Dutasta, J.-P.; Martinez, A. Breathing" Motion of a Modulable Molecular Cavity. *Chem. - Eur. J.* **2017**, *23*, 6495−6498. (b) Martinez, A.; Guy, L.; Dutasta, J.-P. Reversible, Solvent-Induced

Chirality Switch in Atrane Structure: Control of the Unidirectional Motion of the Molecular Propeller. *J. Am. Chem. Soc.* **2010**, *132*, 16733−16734.

(26) (a) Yang, J.; Chatelet, B.; Dufaud, V.; Hérault, D.; Michaud-Chevallier, S.; Robert, V.; Dutasta, J.-P.; Martinez, A. Endohedral Functionalized Cage as a Tool to Create Frustrated Lewis Pairs. *Angew. Chem., Int. Ed.* **2018**, *57*, 14212−14215. (b) Zhang, D.; Jamieson, K.; Guy, L.; Gao, G.; Dutasta, J.-P.; Martinez, A. Tailored Oxido-Vanadium(V) Cage Complexes for Selective Sulfoxidation in Confined Spaces. *Chem. Sci.* **2017**, *8*, 789−794.

(27) (a) Song, J.-R.; Huang, Z.-T.; Zheng, Q.-Y. Synthesis of Functionalized Cyclotriveratrylene Analogues with C1-Symmetry and the Application for 1,4-Michael Addition of Alcohols to Unsaturated Aryl Ketone. *Tetrahedron* **2013**, *69*, 7308−7313. (b) Chakrabarti, A.; Chawla, H. M.; Hundal, G.; Pant, N. Convenient Synthesis of Selectively Substituted Tribenzo[a,d,g]Cyclononatrienes. *Tetrahedron* **2005**, *61*, 12323−12329. (c) Milanole, G.; Gao, B.; Mari, E.; Berthault, P.; Pieters, G.; Rousseau, B. A Straightforward Access to Cyclotriveratrylene Analogues with C_1 Symmetry: Toward the Synthesis of Monofunctionalizable Cryptophanes. *Eur. J. Org. Chem.* **2017**, *2017*, 7091−7100. (d) Lutz, M. R.; Ernst, E.; Zeller, M.; Dudzinski, J.; Thoresen, P.; Becker, D. P. Attempted Resolution and Racemization of Beckmann-Derived CTV-Lactam and the Use of Chirabite-AR® to Determine the Optical Purity of the Supramolecular Scaffold. *Eur. J. Org. Chem.* **2018**, *2018*, 4639−4645. (e) El Ayle, G. G. Ph.D. Thesis, Georgetown University, Washington D.C., 2017.

(28) Collet, A.; Gabard, J.; Jacques, J.; Cesario, M.; Guilhem, J.; Pascard, C. Synthesis and Absolute Configuration of Chiral (C_3) Cyclotriveratrylene Derivatives. Crystal Structure of (M)-(−)-2,7,12-Triethoxy-3,8,13-Tris-[(R)-1-Methoxycarbonylethoxy]-10,15-Dihydro-5H-Tribenzo[a,d,g]-Cyclononene. *J. Chem. Soc., Perkin Trans. 1* **1981**, *0*, 1630−1638.

(29) Canceill, J.; Collet, A.; Gabard, J.; Gottarelli, G.; Spada, G. P. Exciton Approach to the Optical Activity of C_3-Cyclotriveratrylene Derivatives. *J. Am. Chem. Soc.* **1985**, *107*, 1299−1308.

(30) (a) Bruhn, T. S.; Hemberger, A.; Pescitelli, G. *SpecDis version 1.70*; Berlin, Germany, 2017; https://specdis-software.jimdo.com/. (b) Bruhn, T.; Schaumloffel, A.; Hemberger, Y.; Bringmann, G. SpecDis: Quantifying the Comparison of Calculated and Experimental Electronic Circular Dichroism Spectra. *Chirality* **2013**, *25*, 243−249.